

## LASER TRIANGULATION MEASUREMENT OF BLADE OSCILLATION IN A TRANSONIC COMPRESSOR CASCADE

**Petr Šidlof, Pavel Šidlof, Martin Štěpán**  
Technical University of Liberec, NTI FM,  
Studentská 2, Liberec, Czech Republic  
petr.sidlof@tul.cz

**David Šimurda, Jan Lepicovsky**  
Institute of Thermomechanics, Czech Academy of  
Sciences, Dolejškova 5, Prague, Czech Republic

### ABSTRACT

The paper describes a method for optical measurement of oscillation of blades in a linear cascade designed for flutter research. The method uses laser triangulation, which measures the distance between the sensor and the oscillation object. The distance can be recalculated to angular displacement of the blade. However, the relation is nonlinear due to the curvature of the blade. The nonlinear dependence between the distance and angular displacement is derived and quantified analytically. The paper further analyzes the influence of light refraction in the optical window, surface quality and sensor inclination. A procedure for the nonlinear calibration is proposed and used during wind tunnel measurements in a blade cascade with forced oscillation of the middle blade.

### NOMENCLATURE

$f$	frequency of blade oscillation
$M$	inlet Mach number
$n$	refractive index of the optical window
$r$	measured distance
$s$	apparent displacement due to refraction
$t$	thickness of the optical window
$\alpha$	tilt of the incident beam from vertical
$\beta$	tilt of the incident beam from normal
$\varphi$	angular displacement of the blade
$xxA0$	distance of laser spot from the leading edge

### INTRODUCTION

Flow-induced vibration of the blades in front stages of compressors and aft stages or turbines represents a major and persistent concern for their designers and operators. This dangerous phenomenon may lead to catastrophic consequences.

The aeroelastic instability of turbomachinery blades (flutter, non-synchronous vibration, rotating stall) may arise from a number of physical mechanisms. The internal damping in the bladed discs being very low, the critical issue is the aerodynamic damping from unsteady aerodynamic forces, which may be positive (stable) or negative (potentially unstable). The flow-induced vibration may also occur when blade natural frequency locks

in with a specific unstable aerodynamic behavior, such as boundary layer separation, shock wave oscillation or shock wave – boundary layer interaction.

The most common type of aeroelastic instability is flutter. Unlike the classical flutter in external flows, where two structural eigenmodes are coupled due to fluid-structure interaction, flutter in turbomachines is usually related to a single structural mode (Srinivasan, 1997; Ferria, 2011; Chahine, 2019). The stiffness of the blades and the mass ratio is higher than in the case of isolated airfoils, and the flow is usually assumed not to modify the modeshape and frequency.

The tip sections of the long blades in modern large turbomachines often operate under transonic flow regimes. Despite the rapid progress in the CFD techniques and available computational power, transonic flow still represents a challenging regime for contemporary numerical schemes. Experimental data remains indispensable for flutter testing and CFD code validation.

In open literature, there is a number of reports about test facilities for blade flutter research. However, only few dedicated test facilities in the world can operate for transonic flow velocities and reduced frequencies above 0.2. Such facilities are mostly linear cascades, although some semi- or fully-circular cascade facilities have been built. Among the leading research laboratories are EPFL Lausanne in Switzerland (Zanker, 2013), KTH Stockholm in Sweden (Vogt, 2007), TU Darmstadt (Holzinger, 2015) or the NASA Glenn Research Center (GRC) in Cleveland, Ohio, USA (Lepicovsky, 2008). During last three years, a new facility for research of flutter in turbine and compressor blade cascades under transonic flow conditions was designed also in Czech Republic (Lepicovsky, 2021).

The current paper reports on wind tunnel measurements in a transonic blade cascade in this new facility. Specifically, a new optical method for measurement of blade angular displacement is reported, including a nonlinear calibration procedure to enhance its precision.

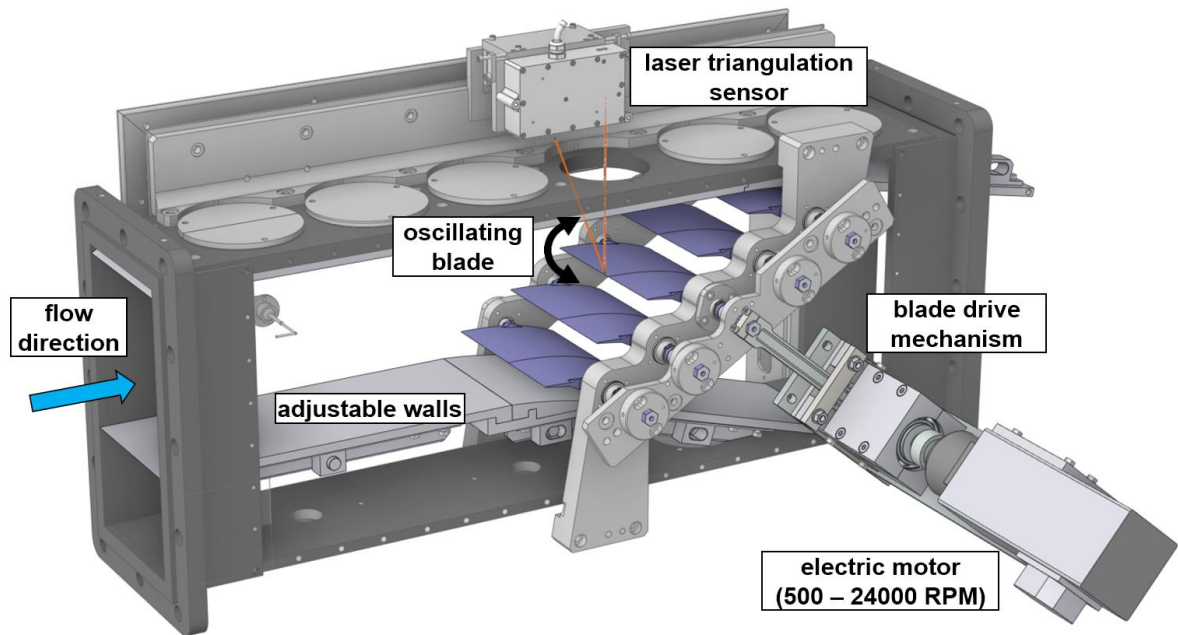


Figure 1. Test section with the laser triangulation sensor.

## EXPERIMENTAL SETUP

The experimental setup consists of a test section mounted in the intermittent suction-type high-speed modular wind tunnel of the Institute of Thermomechanics of the Czech Academy of Sciences (see Figure 1). The test section has an internal cross-section of 160 mm (along the blade span) x 195 mm (height). The blade cascade is composed of five prismatic blades with a profile adopted from a transonic compressor developed at German Aerospace Center (Schreiber & Starken, 1984). The chord length of the profiles is 120 mm, the stagger angle is  $41.49^\circ$  and pitch 74.52 mm. The overall geometry of the cascade is shown in Figure 2.

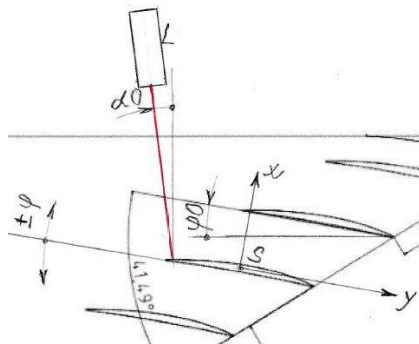


Figure 2. Geometry of the blade cascade (blades No. 2-5) with the laser displacement sensor focused on blade No. 3.

For the measurement of aerodynamic loading, the blades are instrumented with fast-response Kulite pressure transducers. The total torque on the blades is measured by strain gauges mounted on the

blade shaft. Moreover, the flow field can be visualized and measured using shadowgraphy, schlieren or fiber-based digital interferometry. For more details regarding the test section instrumentation and measurement techniques, see (Lepicovsky, 2021) and (Psota, 2021). The current paper focuses mainly on the optical measurement of the blade oscillation using the laser displacement sensor.

The blade drive mechanism can be regarded as kinematic excitation, which imposes torsional harmonic oscillation of the hexagonal shoulder of the blade

$$\varphi(t) = \varphi_a \sin(2\pi f t), \quad (1)$$

where  $\varphi_a$  the angular amplitude and  $f$  the frequency of oscillation. In the current setup, the amplitude at the blade drive shaft has been set to  $\varphi_a = 1^\circ$ . For low frequencies, the blade oscillates as a rigid structure with a constant angular amplitude along the blade span. However, in the case of high-frequency oscillation, the blade undergoes also elastic deformation, whose amplitudes can significantly exceed the rigid body deflections. Thus, it is important to measure the real angular displacement of the blade at least in one point of the blade. For this sake, a fast-response laser triangulation sensor MicroEpsilon ILD 2310-40 was mounted and focused at a point closely downstream the leading edge of the oscillating blade at mid-span. The setting of the sensor, nonlinear calibration and analysis of the accuracy of the measurement is described in the following section.

## OPTICAL MEASUREMENT OF THE BLADE OSCILLATION

The purpose of the measurement is to determine the blade rotation angle (angular deflection) as a function of time. Laser triangulation sensors are currently one of the best methods for this type of measurement. However, the angle of rotation of the blade is a non-linear function of the measured deflection and the accuracy of the measurement is affected by a number of side effects.

The principle of the laser triangulation sensor is measurement of the distance of a laser spot projected on the measured object by angle calculation. The light from the laser diode is focused in the measuring range by special optics. The light reflected from the object is registered by the receiver CCD sensor with additional optics located at a certain angle inside the device. When the distance of the measured object changes, the image moves along the CCD sensor and the built-in processor with a sophisticated program evaluates the distance of the measurement object.

A number of laser triangulation sensors are produced for different distances and measurement ranges. As the object distance increases, the sensor range usually increases, the laser spot diameter increases also and, of course, the sensor resolution, accuracy and linearity decrease.

For the given measurement, a high-end diffusion-type sensor was chosen with a measurement range of 175 to 215 mm (at 49.14 kHz only 195 to 215 mm). The sensor resolution is 2  $\mu\text{m}$ , maximum sampling frequency 49.14 kHz and linearity better than  $\pm 6 \mu\text{m}$ . The diameter of the laser spot is around 0.22 mm. In general, these sensors are among the most stable and reliable for this purpose. However, a number of effects influence accuracy of the measurement the current measurement, namely:

- a) Light refraction when the laser beam passes through the optical window in the upper wall of the wind tunnel
- b) Properties of the measured blade surface (roughness, reflectivity)
- c) Geometry and deformation of the blade
- d) Variations of the angle of incidence of the laser beam on the blade

These effects will be discussed in more detail in the following text.

### Effect of the optical window

The circular perspex glass in the upper wall of the wind tunnel (which is hidden in Figure 1 for clarity) can be considered as a plane-parallel plate, in which the beam refracts twice when it hits at an angle and emerges in a parallel displacement. For the angle of incidence  $\alpha$  (measured from the perpendicular), the plate thickness  $t$  and the refractive index  $n$ , the displacement magnitude  $s$  is

$$s = t \sin(\alpha) \left( 1 - \frac{\cos(\alpha)}{\sqrt{n^2 - \sin^2(\alpha)}} \right). \quad (2)$$

For the given sensor, the refracted laser beam angle lies in the range of approx. 20.9 to 21.3° (for the full sensor range of 40 mm). In the maximum used measurement range of approx.  $\pm 4$  mm, the angle variation is therefore small. The incident beam passes through the plate almost perpendicularly, so there is practically no refraction of light here. However, the reflected oblique beam refracts significantly when passing through the window, and the resulting displacement has a similar effect on the measurement as if the light were coming from a place closer to the sensor (the measured distance is reduced). For an angle of 21° and the refractive index of perspex  $n = 1.6$ , we get  $s = 0.127 t$  and the measured distance decreases by approximately 0.30  $t$ . As the distance of the measured object increases, the incidence angle  $\alpha$  decreases and the displacement  $s$  increases. Therefore, the sensitivity of the sensor increases somewhat. However, the change is small and almost exactly linear.

It can be concluded that measurement with the used triangulation laser sensor through a plane-parallel perspex plate reduces the detected distance in the entire measured range by approximately one third of the thickness of the plate. This has no negative effect, since the measurement is relative and since software offset is performed before each measurement series. At the same time, the sensitivity of the sensor increases slightly (linearly). The change in sensitivity is included in the calibration.

### Properties of the measured blade surface

The ILD 2310-40 sensor is intended for measuring diffusely reflected light. The blade surface has this property to a satisfactory extent. Prescribed blade surface roughness  $R_a = 0.8 \mu\text{m}$  is less than the roughness that, according to the manufacturer, would affect the measurement results of the sensor used.

### Effect of the blade geometry

The measured middle blade performs an oscillating rotational movement around the axis of rotation located approximately in its center. The amplitude at mid-span can reach about  $\pm 4^\circ$ . The movement is measured by the laser sensor L (see Figure 2). The relative rotation angle of the blade  $\varphi$  is determined from the distance  $r$  measured by the sensor. The position of the sensor is defined by the  $x$ -distance between the laser spot and the leading edge in the neutral blade position (for  $\varphi = 0$ ), and by the angle  $\alpha_0$ . The sensor is usually placed vertically ( $\alpha_0 = 0$ ). For the purpose of the calculation, the coordinate system  $(x,y)$  with origin  $S$  in the axis of rotation is aligned with the blade. The blade profile is specified in the  $(xx,yy)$  system, which is parallel to

the  $(x,y)$  system, and its origin  $S_0$  at the top of the entering edge has coordinates  $x_0, y_0$ .

The geometric scheme for the calculation is shown in Fig. 3. Since the  $(x,y)$  system is fixed with the blade, the measuring system (laser sensor and its beam) rotates relative to the blade in the opposite direction, i.e. counter-clockwise. For the rotation angle  $\varphi = 0$ , the laser beam  $r_0$  starts at  $B_0$  and hits the blade at  $A_0$ . When the blade rotates by an angle  $\varphi$ , points  $B_0, A_0$  move to  $B, A_r$ . The line  $B-A_r$ , which is the carrier of the laser beam, intersects the blade profile at point  $A$ . The distance  $r$  between the points  $B$  and  $A$  represents the theoretical result of the distance measurement for the angle  $\varphi$ .

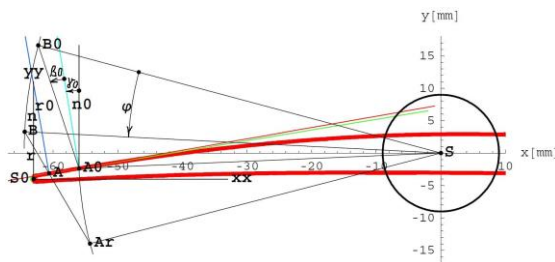


Figure 3. Geometric scheme for the calculation.

The deviation  $\beta_0$  of the laser beam from the normal to blade surface is important to assess the measurement errors caused by the oblique incidence of the beam. The normal  $n_0$  forms an angle  $\gamma_0$  with the  $y$  axis. The deviation  $\beta_0$  also depends on the angle  $\alpha_0$  between the laser beam and vertical (Figure 2). Since  $\alpha_0 + \varphi_0 = \beta_0 + \gamma_0$ ,  $\beta_0 = \alpha_0 + \varphi_0 - \gamma_0$ . When rotated by  $\varphi$ ,  $\beta_0$  changes to  $\beta = \alpha_0 + \varphi + \varphi_0 - \gamma$ , where  $\gamma$  is the angle of the normal to the blade profile at point  $A$ . Since  $\gamma$  changes little in the measurement range used, the angle  $\beta$  of the beam incidence on the blade is approximately proportional to  $\varphi$ . The situation is demonstrated in Figure 3 for  $\beta_0 = 9^\circ$ ,  $\varphi = 12^\circ$ ,  $xxA_0 = 7$  mm,  $r_0 = 20$  mm,  $x_0 = -63$  mm and  $y_0 = -4$  mm, which results in  $r = 7.47$  mm,  $\beta = 20.45^\circ$ ,  $xxA = 2.39$  mm,  $\gamma_0 = 9.35^\circ$  and  $\gamma = 9.9^\circ$ .

To assess the degree of nonlinearity between the angle of rotation  $\varphi$  and distance  $r$  measured by the laser displacement sensor, an analytical calculation was performed. The calculation consists of five stages:

1. Approximation of the shape of the suction side of the blade near the leading edge in coordinate system  $(xx, yy)$  by a 2<sup>nd</sup> degree polynomial  $yVa_0[xx] = aL \ xx^2 + bL \ xx + cL$  (accuracy 0.5  $\mu$ m)
2. Transformation of  $yVa_0[xx]$  to  $yVa[x]$ , determination of coordinates of points  $A_0, B_0$  (from  $xxA_0, r_0, \beta_0$ ) and rotation of points  $A_0, B_0$  to  $A_r, B$ .

3. Calculation of the intersection point  $A$  of line  $A_r-B$  with the curve  $yVa[x]$ , defined by the coordinate  $x\varphi[\varphi]$
4. Calculation of  $\beta[\varphi]$  as the angle between the laser beam  $r$  and the normal to blade surface at point  $A$
5. Calculation of  $r[\varphi]$  as the distance between points  $B, A$ .

The function  $r[\varphi]$  is relatively complicated and the inverse function  $\varphi[r]$  cannot be explicitly derived. Therefore, an approximate function of three variables  $rFit[\varphi, xxA_0, \alpha_0]$ , was calculated by linear regression. The inaccuracy of this approximation does not exceed  $\pm 0.01$  mm within certain limits of the variables. This function can be readily inverted.

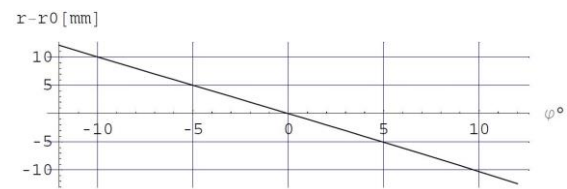


Figure 4. Calculated dependence between the distance and rotation angle for  $\alpha_0 = 0^\circ$ ,  $\beta_0 = 0.41^\circ$  and  $xxA_0 = 5$  mm

Figure 4 shows the calculated dependence between the distance  $r$  and rotation angle  $\varphi$  for a commonly used sensor setup. Visually, the relation is almost perfectly linear and the proportionality constant is close to one. To quantify the deviation from linearity, the difference of the function displayed in Figure 4 and its linear approximation is shown in Figure 5 for four positions of the laser spot  $xxA_0$ . It can be seen that when the blade rotates between  $\pm 4^\circ$ , a linear approximation would introduce an error of up to 0.06 mm (i.e., up to  $0.06^\circ$ ). The distance  $xxA_0$  of the laser spot from the leading edge of the blade has only minor influence.

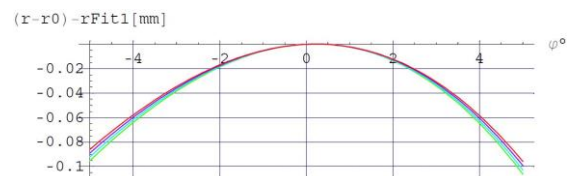
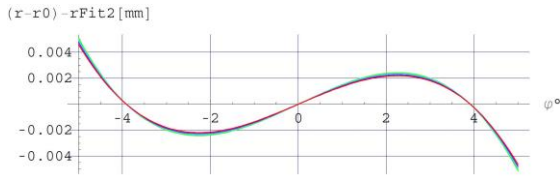


Figure 5. Calculated error of the linear approximation ( $\alpha_0 = 0^\circ$ ,  $xxA_0 = 2$  to 8 mm, green to red)

Figure 6 shows the calculated inaccuracy when a quadratic approximation  $r(\varphi)$  is used. In this case, the error is reduced by an order of magnitude and does not exceed 0.002 mm ( $0.002^\circ$ ) within the measured range.



**Figure 6. Calculated error of the quadratic approximation ( $\alpha\theta = 0^\circ$ ,  $x_{xA0} = 2$  to  $8$  mm, green to red)**

### Effect of the sensor inclination

From the documentation of the manufacturer, it follows that tilt angles of the target in diffuse reflection both around the X and the Y axis of less than  $5^\circ$  only have a disturbing effect with surfaces which are highly reflecting. For tilt angles in the  $\pm 5^\circ$  range, the specified error is less than 0.12% of the range, i.e. in our case 0.024 mm. By choosing the appropriate setting of the sensor so that the angle  $\beta$  (deviation of the beam from the normal, which follows from the calculation) is within the smallest possible limits, the error can be reduced to less than 0.01 mm. Moreover, if a nonlinear calibration of the sensor is performed, this adverse effect can be compensated within the calibration to high extent.

### CALIBRATION OF THE SENSOR

The analytic derivations and results summarized in the previous chapter can be used for calibration of the laser triangulation sensor. A set of measurements of the blade angular displacement (measured by a digital water-level) and distances (measured by the laser triangulation sensor) was recorded in the range  $\varphi = -3.5^\circ \dots 3.5^\circ$ . The calibration points are shown in Figure 7 together with a linear and quadratic approximation.

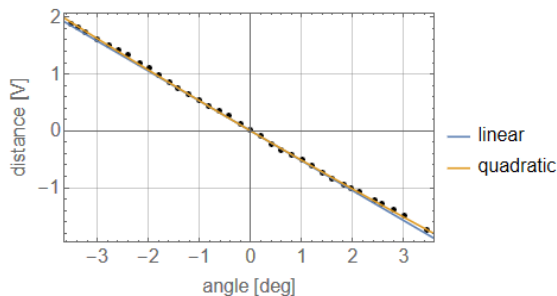


**Figure 6. Measured calibration points, linear and quadratic regression curves.**

Figure 7 displays the residuals of the linear and quadratic regression curves. The residuals do not quantify directly the accuracy of the approximation, since the calibration points are scattered due to measurement errors (especially the precision of the digital water-level, which is about  $0.01^\circ$ ). Yet, it can be seen that the peak residuals of the quadratic approximation are two to three times lower than those of the linear approximation, and likely more if

the calibration points were taken in the same range  $\varphi = -4^\circ \dots 4^\circ$  as the analytical derivations.

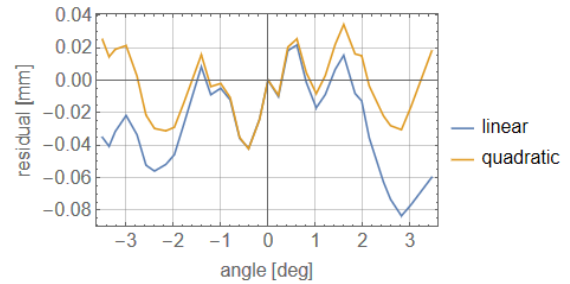


**Figure 7. Residuals of the linear and quadratic regression curves.**

### BLADE OSCILLATION MEASUREMENTS

The calibrated signal from the laser triangulation sensor was used in a series of wind tunnel measurements with an oscillating blade, where the blade angular position is the primary variable and the blade surface pressure measurements, strain gauge and wake measurements must be interpreted as a function of the blade position. These results were published e.g. in (Lepicovsky, 2021) or (Lepicovsky, 2022). In this contribution, the angular displacement measurements are shown for a still-air configuration ( $M = 0$ ) in Figure 8 and for a transonic flow with inlet Mach number  $M = 1.09$  in Figure 9.

In the case of low frequency  $f = 10$  Hz, the blade oscillates as a rigid structure with an angular amplitude close to  $1^\circ$ , which corresponds to the prescribed amplitude of the kinematic excitation by the blade drive mechanism. At higher frequencies, the blade also deforms elastically in addition to the rigid oscillation, with the total amplitude of up to  $2.3^\circ$  at mid-span.

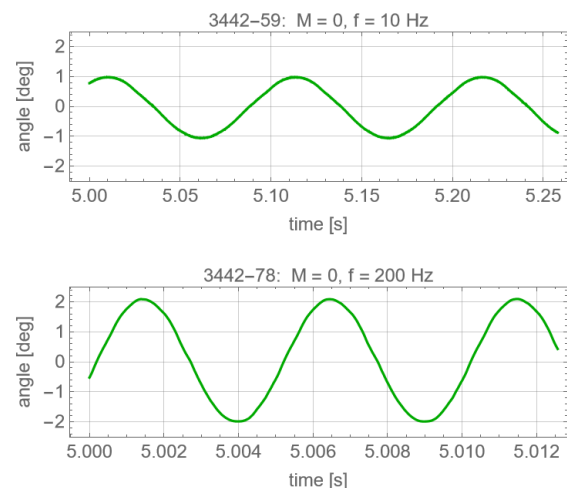


**Figure 8. Angular displacement of the oscillating blade in still-air configuration ( $M = 0$ ), oscillation frequency  $f = 10$  Hz and  $f = 200$  Hz**

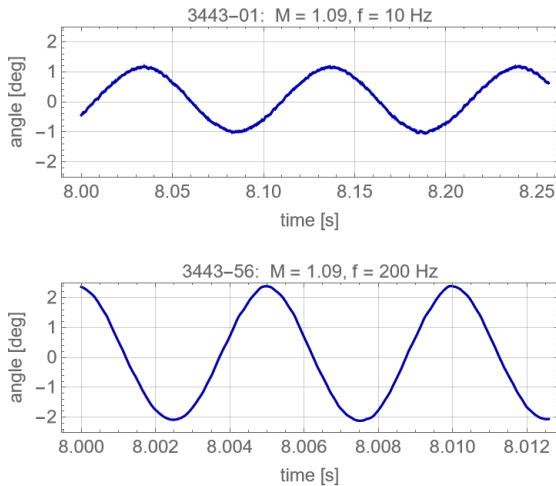


**Figure 9. Angular displacement of the oscillating blade for inlet Mach number  $M = 1.09$ , oscillation frequency  $f = 10$  Hz and  $f = 200$  Hz**

The amplitude of the angular displacement as a function of blade oscillation frequency is shown in Figure 10 both for the still-air and transonic case. Because the inertial moment scales with the square of the oscillation frequency, the amplitudes increase quickly. As the frequency approaches the first natural frequency of the blade, which is  $f_1 = 267$  Hz, the amplitudes rise even faster than quadratically. In the transonic case, the oscillation amplitudes are about 10-15% higher than in the still-air configuration. This corresponds to the ratio between the inertial and aerodynamic forces.

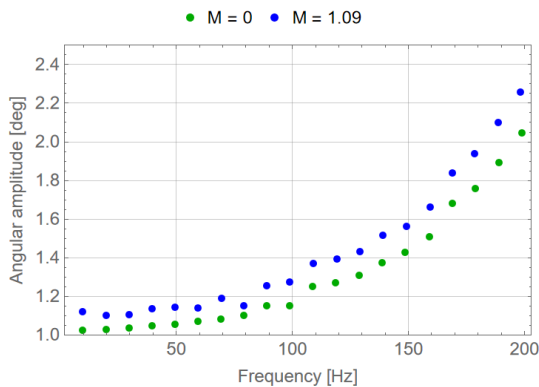


**Figure 10. Oscillation amplitude as a function of frequency for the still-air configuration and**

## DISCUSSION AND CONCLUSIONS

For the sake of angular oscillation measurement of a curved blade within a project focused on experimental research of flutter in turbomachinery, an optical method using a fast-response laser triangulation sensor has been developed. The device measures the linear distance between the sensor and the rotating blade along a fixed line, which means that the laser spot moves chordwise when the blade rotates. Thus, the measured distance is a complicated weakly nonlinear function of the

angular displacement. For the given geometry, a mathematical model of this function was derived. The function was approximated by polynomials of the first, second and third order. It was shown that a quadratic function improves the accuracy by an order of magnitude compared to a simple linear fit.

The analytic relations derived in this study could be theoretically used to calculate the angular displacement from the distance measured by the laser triangulation sensor directly. However, a number of further parameters, which are difficult to be measured accurately, need to be specified (e.g. the inclination  $\alpha\theta$  of the sensor, precise location  $xxA\theta$  of the laser spot, but also refraction effects caused by the optical window as described above). This makes this option impractical.

Nevertheless, the results obtained from the computational model lead to clear guidelines and quantitative indications, how a calibration of the blade angular displacement measurement should be performed:

- The laser displacement sensor should be aligned so that the incident beam is normal to the blade surface in its mean position.
- The ideal position of the laser spot is about 2 mm from the leading edge of the blade. In this configuration, the previous condition is satisfied when the laser beam is vertical, the proportionality constant between the distance and angle is close to one and inaccuracy of the quadratic approximation is low.
- After each reassembly, where the position of the sensor and laser spot may change, a calibration should be performed by registering a set of blade angular deflections  $\varphi$  and measurements from the laser displacement sensor  $r$ .
- The calibration points should be approximated by a quadratic curve  $r(\varphi)$ , i.e. by a square-root function  $\varphi(r)$ . This calibration can be then used during the measurements

It has been shown that using a simple linear calibration can introduce an error of angular deflection measurement up to 0.05 deg for an ideally aligned setup, and up to 0.1 deg if the laser beam is not perfectly vertical. When a quadratic (square-root) fit is used, the error is reduced by an order of magnitude. Following the procedure explained above, the linear displacement sensor can be used to measure the angular displacements of the curved blade without compromising the accuracy of the sensor.

The quantitative data reported in this paper hold only for the specified profile and blade cascade geometry. However, the qualitative recommendations are valid generally and with the methods developed, the same derivation can be readily reiterated for any geometry.

## ACKNOWLEDGMENTS

The research was supported by the Ministry of Education, Youth and Sports of the Czech Republic, project No. LTAUSA19036 *Advanced experimental research on synchronous and non-synchronous blade vibration*.

Off-Design Conditions, *Journal of Engineering for Gas Turbines and Power* **129**(2), pp. 530–541.

Zanker A., Ott P., Calza P. (2013) Experimental Aeroelastic Analysis of Clustered Turbine Blades Vibrating in Mixed Torsion/Bending Mode, *31st AIAA Applied Aerodynamics Conference*, 3152

## REFERENCES

Chahine C., Verstraete T., He L. (2019), A comparative study of coupled and decoupled fan flutter prediction methods under variation of mass ratio and blade stiffness, *Journal of Fluids and Structures* **85**, pp. 110–125.

Ferria H. (2011), Contribution to Numerical and Experimental Studies of Flutter in Space Turbines. Aerodynamic Analysis of Subsonic or Supersonic Flows in Response to a Prescribed Vibratory Mode of the Structure, Ph.D. thesis, Ecole Centrale de Lyon, KTH Stockholm.

Fürst J., Lasota M., Lepicovsky J., Musil J., Pech J. et al. (2021), Effects of a Single Blade Incidence Angle Offset on Adjacent Blades in a Linear Cascade, *Processes* **9**(11), pp. 1974.

Holzinger F., Wartzek F., Schiffer H.-P., Leichtfuss S., Nestle M. (2015), Self-Excited Blade Vibration Experimentally Investigated in Transonic Compressors: Acoustic Resonance, *Journal of Turbomachinery* **138**(4).

Lepicovsky J. (2008), Investigation of flow separation in a transonic-fan linear cascade using visualization methods, *Experiments in Fluids* **44**(6), pp. 939–949.

Lepicovsky J., Šidlof P., Šimurda D., Štěpán M., Luxa M. (2021), New test facility for forced blade flutter research, *AIP Conference Proceedings*, pp. 030001

Lepicovsky J., Šimurda D., Šidlof P., Luxa M. (2022), A simplified method for approximate determination of blade flutter aerodynamic loading function, *ASME Turbo Expo 2022*, GT2022-83351

Psota P., Čubrelí G., Hála J., Šimurda D., Šidlof P. et al. (2021), Characterization of Supersonic Compressible Fluid Flow Using High-Speed Interferometry, *Sensors* **21**(23), pp. 8158.

Šidlof P., Vlček V., Štěpán M. (2016), Experimental investigation of flow-induced vibration of a pitch-plunge NACA 0015 airfoil under deep dynamic stall, *Journal of Fluids and Structures* **67**, pp. 48–59.

Schreiber, H.A. and Starke, H. (1984), Experimental Cascade Analysis of a Transonic Compressor Rotor Blade Section”, *J. of Eng. for Gas and Power*, **106**, pp. 288–294.

Srinivasan A. V. (1997), Flutter and Resonant Vibration Characteristics of Engine Blades, *ASME Turbo Expo: Power for Land, Sea and Air, Volume 4*.

Vogt D. M., Fransson T. H. (2007), Experimental Investigation of Mode Shape Sensitivity of an Oscillating Low-Pressure Turbine Cascade at Design and